

Magnetic Properties of Free Cobalt Clusters

J. P. Bucher, D. C. Douglass, and L. A. Bloomfield

Department of Physics, University of Virginia, Charlottesville, Virginia 22901

(Received 8 February 1991)

We have studied the magnetic properties of cobalt clusters in a beam as functions of cluster size ($N=20-200$), magnetic field, and cluster temperature. The measured magnetic moments per atom increase with applied magnetic field and cluster size but decrease with increasing temperature, consistent with superparamagnetic behavior. Rapid orientation fluctuations of the true magnetic moments of these isolated particles yield the smaller, time-averaged, observed values. The true magnetic moments are $(2.08 \pm 0.20)\mu_B$ per atom and exceed the bulk value. Magnetically resolved isomers are seen for $N=55-66$.

PACS numbers: 75.50.Cc, 36.40.+d

While bulk magnetic properties of ferromagnetic materials have been widely studied and are relatively well understood, experimental work on the finely divided states of these materials is in its early stages and only a handful of experiments have been performed on unsupported ferromagnetic clusters.¹⁻³ Cluster studies provide important means for examining the effects of system size, temperature, and other physical parameters on spatial and magnetic order and should contribute to a better understanding of the nature of the interactions responsible for magnetism.

Recent results on magnetic deflection of ferromagnetic particles in a beam^{2,3} have raised some controversy, since the clusters deflect only toward increasing magnetic field with magnetic moments per atom that appear to be much smaller than the expected theoretical values.⁴⁻⁹ While we continue to measure small magnetic moments, we find that all attempts at obtaining colder clusters, whether by decreasing the cluster source temperature, increasing the thermalization time within the source, or raising the density of cooling gas in the source, lead to increases in the measured magnetic moments of the clusters. This result conflicts with a previous report that magnetic moments increase with cluster internal temperature.²

Our measurements agree quantitatively with the predictions of superparamagnetism, in which the small measured magnetic moments are the time-averaged projections of much larger true moments onto the applied magnetic field. Rapid fluctuations in the orientations of the true moments produce time-averaged values that are nonzero only in the presence of applied magnetic fields. The increase in the measured magnetic moment per atom with increasing magnetic field, increasing cluster size, and decreasing temperature all reflect the thermal character of the orientation fluctuations. Despite the limitations imposed by these finite-temperature effects, we have also identified structural isomers that have significantly different magnetic moments.

The experimental technique couples the conventional Stern-Gerlach deflection scheme with modern pulsed-

laser-vaporization source technology and time-of-flight mass spectrometry.¹ Our experimental setup has been described elsewhere,³ and only a brief description will be given here. The apparatus consists of two vacuum chambers that produce the collimated cluster beam, a gradient magnet and flight tube in which the beam is deflected, and a final chamber in which the masses of the clusters and their deflections are analyzed.

Cobalt clusters are produced in the first chamber by laser vaporization of a sample. A pulsed Nd-doped yttrium-aluminum-garnet laser evaporates cobalt from a translating and rotating sample disk into a 0.5-cm³ cavity, filled with helium gas by a pulsed valve. The cavity opens into the vacuum through a cylindrical nozzle, 1.6 mm in diameter. The source operates at 10 Hz with a He backing pressure of 5 bars. The whole source assembly, including the modified General Valve valve and its helium-gas reservoir,¹⁰ can be coupled thermally to a liquid-nitrogen reservoir and cooled to 77 K.

The carrier-gas-cluster mixture undergoes a free-jet expansion into the vacuum, producing a supersonic cluster beam. This beam passes a first skimmer and enters the second chamber, where it is collimated through a razor-blade skimmer followed by a planar slit into a narrow beam, 0.8 mm wide by 2.5 mm high. The collimated beam then passes through a gradient-magnet assembly where the clusters are deflected according to the projections of their magnetic moments onto the field axis. To achieve optimal field gradient homogeneity, the 250-mm-long pole faces of the magnet reproduce a quadrant of a quadrupolar field.¹¹ The field is formed by a hyperbolic bead that is suspended down the center of a 90° groove. The absolute value of the field increases linearly as a function of the radius when going from the bottom of the groove to the bead. The field and field gradient inside the magnet were calibrated with a Hall probe magnetometer.

The clusters travel from the magnet to the third chamber through a flight tube and are finally ionized, 2.770 m downstream from the source, by a narrowly collimated pulsed ultraviolet beam (193 nm) from an ArF

excimer laser. The laser light (0.8 mm \times 5 mm) can be scanned through the cluster beam to measure the Stern-Gerlach profile of the deflected clusters. The cluster ions are mass analyzed by means of a time-of-flight mass spectrometer (TOFMS) with dual microchannel plates as its detector.

The velocities of the clusters are measured with the help of a chopper wheel installed in the second chamber. The chopper slit permits only a brief packet of clusters to pass through the wheel and establishes an exact starting time for this cluster packet. The exact arrival time in the acceleration region of the TOFMS is set by the ionizing laser pulse. From the flight time between chopper and TOFMS, we can determine the velocity of the clusters and can extrapolate back to find the time at which they left the source. Thus we can accurately calculate the time τ_{res} the clusters resided in the source, between the moment of vaporization and the moment they left the source nozzle. The chopper is always used in connection with data collection so that no auxiliary experiment is needed to determine the velocities or source residence times of the clusters.

The cobalt clusters deflect exclusively toward increasing magnetic field. The clusters of a given mass deflect by as much as several mm with no significant increase in the spatial width of the beam. Knowing a cluster's velocity v_x , its mass, and the deflection it experiences due to passage through the gradient magnet, we can calculate its measured magnetic moment per atom, μ_{expt} .

As we mentioned previously,³ the residence time τ_{res} of a cluster in the source can be quite long and is often a substantial fraction of the time between the vaporization laser pulse and the ionization pulse at the TOFMS. The remaining time is flight time through the apparatus and depends on the velocity of the cluster. Using the chopper wheel, we can distinguish between cluster-velocity v_x and source-residence-time τ_{res} effects on μ_{expt} . We find that μ_{expt} is relatively insensitive to the velocity v_x of the clusters (for constant source conditions) but depends strongly on τ_{res} , leading us to conclude that the residence time also plays the key role in defining the cluster temperature.

Figure 1 shows μ_{expt} as a function of the number N of atoms per cluster for a source cooled to liquid-nitrogen temperature. Only particles with a specific residence time and a specific velocity were used. Three size ranges were explored by making slight changes in the preexpansion carrier-gas density. Judging from the satisfactory overlap between different size ranges, this technique seems to come very close to the constant-temperature condition, although we find that large increases in the preexpansion helium density will increase μ_{expt} slightly, an effect we attribute to improved cooling of the clusters.

In Fig. 1, we notice a linear increase of μ_{expt} with cluster size for the clusters $N < 55$ and again for $N > 66$, although the slopes in the two regions are somewhat different. The fine structure is within the error bars of the

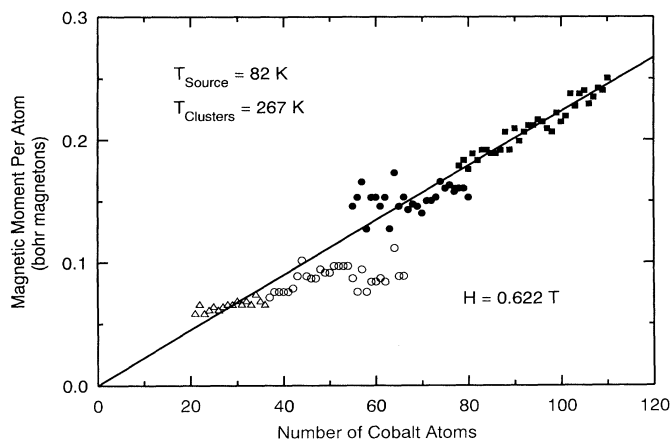


FIG. 1. Measured magnetic moment per atom, μ_{expt} , as a function of cluster size, for a source temperature of 82 ± 1 K and $H = 0.622$ T. These particles had a translational velocity $v_x = (0.610 \pm 0.012) \times 10^3$ m/s and a residence time $\tau_{\text{res}} = 850$ μ s. The carrier gas density is increasing in the order Δ , \circ , \bullet , and \blacksquare . The velocity of the He carrier gas, $v_{\text{He}} = (0.96 \pm 0.03) \times 10^3$ m/s, was measured with a fast ionization gauge (Ref. 10). Two deflection peaks (\circ and \bullet) are observed for $N = 55$ – 66 , except at $N = 63$ where only a single broad peak is seen. The solid curve is a plot of μ_{eff} from Eq. (1) for a cluster temperature of 267 K.

measurement. On the other hand, the region around $N = 55$ is quite complicated. This particular size corresponds to a shell closing of both the cubo-octahedral and the icosahedral structures. In fact, the deflection profiles of $N = 55$ – 66 contain two maxima and most probably indicate the coexistence in the cluster beam of two isomers that exhibit magnetic moments differing by approximately a factor of 2. These features are fully reproducible within the accuracy of our measurements (typically $\pm 8\%$ of the measured magnetic moment). As the cluster size increases, the low-magnetic-moment deflection peak gradually disappears and the high-magnetic-moment peak gradually becomes visible. We suspect that a low-moment isomeric sequence, dominant for $N < 55$, vanishes by $N = 67$ and is replaced by a high-moment isomeric sequence that first appears around $N = 55$. The differences in magnetic moments between the isomeric sequences are substantial enough that complete structural rearrangements may be required to explain them. Calculations of the effects of cluster symmetry on magnetic moments indicate that a change in basic cluster symmetry could account for these observations.⁹ Other sizes may display isomer effects but individual structures cannot yet be resolved and lead mainly to a broadening of the deflection profiles.

Figure 2 shows the dependence of μ_{expt} on applied magnetic field H for three different cluster sizes emitted by the liquid-nitrogen-cooled source. For each size, μ_{expt} increases almost linearly as a function of field.

Figure 3 shows μ_{expt} for a wide range of cluster sizes

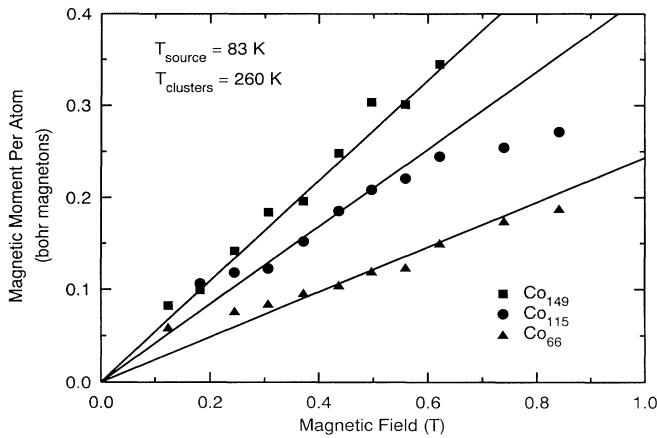


FIG. 2. Measured magnetic moment per atom, μ_{expt} , as a function of field for several cluster sizes, for a source temperature of 83 ± 1 K. μ_{expt} for a given N is calculated from an average over five mass peaks ($N-2$ to $N+2$). $\tau_{\text{res}} = 850 \mu\text{s}$, $v_x = (0.610 \pm 0.012) \times 10^3$ m/s, and $v_{\text{He}} = (0.96 \pm 0.03) \times 10^3$ m/s. The solid curves are plots of μ_{eff} from Eq. (1) for a cluster temperature of 260 K.

and two different source temperatures. Cooling the source dramatically increases μ_{expt} . In fact, the magnetic field had to be reduced for the cold-source measurements because a 0.966-T field deflected the larger clusters out of the mass spectrometer and into the magnet's pole faces. This increase in μ_{expt} with decreasing source temperature suggests finite-temperature effects are responsible for the smallness of the measured magnetic moments.

The results of Figs. 1–3 differ from theoretical expectations for two important reasons. First, the magnetic moments per atom are expected to be relatively insensitive to cluster size, applied magnetic field, and any temperature that is well below the bulk cobalt Curie temperature of 1404 K. Instead, μ_{expt} depends strongly on all three physical parameters. Second, while theory predicts that the magnetic moment per atom in small clusters should equal or exceed the bulk value of $1.72\mu_B$ per atom, μ_{expt} is always substantially less than this value.

To improve our understanding of the effects of cluster temperature on the measured magnetic moment per atom, μ_{expt} , we studied μ_{expt} for $N=115$ as a function of residence time τ_{res} (see Fig. 4). The saturation of μ_{expt} for residence times longer than 1.6 ms indicates that the internal temperatures of the clusters are in equilibrium with the source at 83 K. Under these circumstances, the clusters are grown and thermalized during the time when the He-gas pulse is most intense ($500 \mu\text{s}$) and they leave the source cavity together with the trailing edge of the carrier-gas pulse. The saturation value, $\mu_{\text{expt}} = 0.402\mu_B$ per atom, is the largest measured magnetic moment per atom obtainable in a 115-atom cobalt cluster for this source temperature (83 K) and this applied magnetic field (0.307 T). Adjustments in the free-jet-expansion

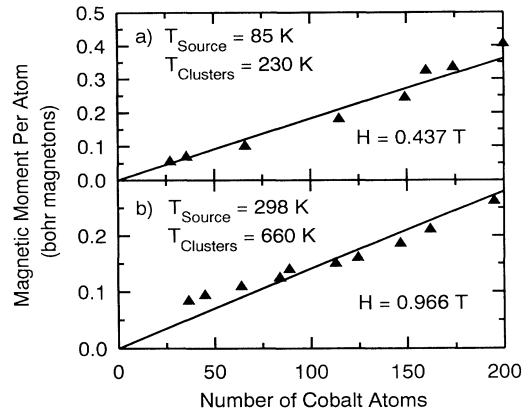


FIG. 3. Measured magnetic moment per atom, μ_{expt} , as a function of cluster size, for (a) a source temperature of 85 ± 1 K and $H = 0.437$ T and (b) a source temperature of 298 K and $H = 0.966$ T. The magnetic moment for a given N is calculated from an average over five mass peaks ($N-2$ to $N+2$). For (a), $\tau_{\text{res}} = 850 \mu\text{s}$, $v_x = (0.610 \pm 0.012) \times 10^3$ m/s, and $v_{\text{He}} = (0.96 \pm 0.03) \times 10^3$ m/s. For (b), $\tau_{\text{res}} = 320 \mu\text{s}$, $v_x = (1.04 \pm 0.02) \times 10^3$ m/s, and $v_{\text{He}} = (1.76 \pm 0.04) \times 10^3$ m/s. The solid curves are plots of μ_{eff} from Eq. (1) for cluster temperatures of (a) 230 K and (b) 660 K.

conditions did not significantly affect μ_{expt} . Unfortunately, working with longer residence times significantly decreases the cluster signal. This technical constraint lead us to use shorter residence times for the bulk of our measurements.

Since a detailed treatment of finite-temperature magnetism of transition-metal clusters is not yet available, we can discuss the experimental results using simple models only. Two such models have recently been proposed. Merikowski *et al.*¹² suppose that the reduction in measured magnetic moment is due to intraparticle temperature-induced spin disorder. Using a Monte Carlo approach to study an Ising (1) model, they find that very high internal temperatures should be able to reduce the cluster magnetic moments to the observed values.

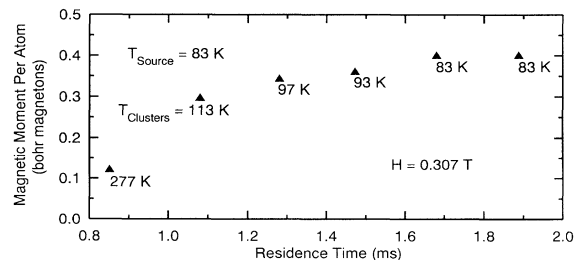


FIG. 4. Measured magnetic moment per atom, μ_{expt} , as a function of residence time for $N=115$ atom clusters. The source temperature is 83 ± 1 K, $H = 0.307$ T, and $v_x = (0.630 \pm 0.012) \times 10^3$ m/s. Values of cluster temperature T_{clusters} were obtained from Eq. (1) by assuming that the rightmost point is in thermal equilibrium with the source.

Khanna¹³ proposes that the clusters are superparamagnetic particles (monodomain particles) where the directions of their magnetic moments fluctuate rapidly under thermal agitation, as they would do above the blocking temperature in a granular composite,¹⁴ suspended particle,¹⁵ or dilute magnetic alloy.¹⁶ The clusters' internal temperatures are high enough to permit their magnetic moments to orient independently of their atomic lattices. During the several hundred microseconds it spends in the magnet, the true magnetic moment of each particle explores much of the Boltzmann distribution of magnetic moment projections on the field axis, yielding the Langevin function for the time-averaged magnetic moment per atom μ_{eff} :

$$\mu_{\text{eff}} = \mu \left[\coth \left(\frac{N\mu H}{k_B T} \right) - \frac{k_B T}{N\mu H} \right], \quad (1)$$

where μ is the true magnetic moment per atom of the particle. Fluctuations occur on the nanosecond time scale, with the magnetic moment exchanging angular momentum with the particle's lattice through crystal anisotropy couplings and energy with the particle's vibrational modes. The large vibrational heat capacity establishes the temperature of the particle.

Khanna's picture is consistent with our own Monte Carlo studies of the classical Heisenberg Hamiltonian for cubo-octahedral particles.¹⁷ In the latter work, we find that, at our experimental temperatures, the particles should indeed be almost entirely superparamagnetic, with large magnetic moments that fluctuate significantly in direction but only slightly in magnitude. Both Khanna's results and our own calculations predict the observed linear increases of measured magnetic moment with cluster size and magnetic field and the decrease in the measured moment with increased temperature. Setting μ_{eff} equal to μ_{expt} from Fig. 4 at saturation, $N=115$, $H=0.307$ T, and $T=83$ K, Eq. (1) yields $\mu=(2.08 \pm 0.20)\mu_B$ per atom. This value is more than the bulk value of $1.72\mu_B$ per atom. Theoretical curves based on Eq. (1) and $\mu=2.08\mu_B$ per atom appear in Figs. 1-3. In these curves, the cluster internal temperature T_{clusters} is the only adjustable parameter. Equation (1) was also used to obtain T_{clusters} for the shorter τ_{res} points in Fig. 4. Most of the cold-source data were taken with $\tau_{\text{res}}=850$ μs , when the clusters have an internal temperature of approximately 277 K. The quantitative agreement between the superparamagnetic model and the measured magnetic behavior leads us to conclude that

cobalt clusters are indeed superparamagnetic with true magnetic moments per atom in excess of the bulk value.

Our measurements also indicate that clusters produced by laser-vaporization sources are likely to be very hot and that supersonic expansions are not necessarily able to cool their vibrational temperatures effectively. Nonetheless, we have shown that they can be brought into thermal equilibrium with the source by keeping them inside for several milliseconds and that their temperatures can be measured accurately if they exhibit superparamagnetic behavior.

The authors wish to thank S. N. Khanna, P. Jena, and B. I. Dunlap for many helpful discussions. We also gratefully acknowledge technical support from B. Haynes and P. Xia. This work is supported by ONR Contract No. N00014-88-K-0422. J.P.B. gratefully acknowledges support from the Swiss National Science Foundation, Grant No. 8220-025964.

¹D. M. Cox, D. J. Trevor, R. L. Whetten, E. A. Rohlfing, and A. Kaldor, *Phys. Rev. B* **32**, 7290 (1985).

²W. A. de Heer, P. Milani, A. Chatelain, *Phys. Rev. Lett.* **65**, 488 (1990).

³J. P. Bucher, D. C. Douglass, P. Xia, B. Haynes, and L. A. Bloomfield, *Z. Phys. D* (to be published).

⁴C. Y. Yang, K. H. Johnson, D. R. Salahub, J. Kaspar, and R. P. Messmer, *Phys. Rev. B* **24**, 5673 (1981).

⁵K. Lee, J. Callaway, K. Kwong, R. Tang, and A. Ziegler, *Phys. Rev. B* **31**, 1796 (1985).

⁶A. Rosen and T. T. Rantala, *Z. Phys. D* **3**, 205 (1986).

⁷F. Liu, M. R. Press, S. N. Khanna, and P. Jena, *Phys. Rev. B* **39**, 6914 (1989).

⁸G. M. Pastor, J. Dorantes-Davila, and K. H. Bennemann, *Phys. Rev. B* **40**, 7642 (1989).

⁹B. I. Dunlap, *Phys. Rev. A* **41**, 5691 (1990).

¹⁰J. P. Bucher, D. C. Douglass, P. Xia, and L. A. Bloomfield, *Rev. Sci. Instrum.* **61**, 2374 (1990).

¹¹D. McColm, *Rev. Sci. Instrum.* **37**, 1115 (1966).

¹²J. Merikowski, J. Timonen, M. Manninen, and P. Jena, *Phys. Rev. Lett.* **66**, 938 (1991).

¹³S. N. Khanna (to be published).

¹⁴G. Xiao, S. H. Liou, A. Levy, J. N. Taylor, and C. L. Chien, *Phys. Rev. B* **34**, 7573 (1986).

¹⁵T. Furubayashi and I. Nakatani, *Solid State Commun.* **74**, 821 (1990).

¹⁶J. Korecki and K. Krop, *Surf. Sci.* **106**, 444 (1981).

¹⁷L. A. Bloomfield and J. P. Bucher (to be published).